# Prediction of Hepatocellular Carcinoma by Liver Stiffness Measurements Using Magnetic Resonance Elastography After Eradicating Hepatitis C Virus

Takashi Kumada, MD, PhD[1], Hidenori Toyoda, MD, PhD[2], Satoshi Yasuda, MD, PhD[2], Yasuhiro Sone, MD, PhD[3], Sadanobu Ogawa[4], Kenji Takeshima[4], Toshifumi Tada, MD, PhD[5], Takanori Ito, MD, PhD[6], Yoshio Sumida, MD, PhD[7] and Junko Tanaka, PhD[8]

INTRODUCTION: **Liver fibrosis stage is one of the most important factors in stratifying the risk of developing hepatocellular carcinoma (HCC). We evaluated the usefulness of liver stiffness measured by magnetic resonance elastography (MRE) to stratify the risk of developing HCC in patients who underwent MRE before receiving direct-acting antivirals (DAAs) and subsequently achieved sustained virological response (SVR).**

METHODS: **A total of 537 consecutive patients with persistent hepatitis C virus who underwent initial MRE before DAA therapy and achieved SVR were enrolled. Factors associated with HCC development were analyzed by univariate and multivariate Cox proportional hazards models.**

RESULTS: **Albumin-bilirubin score ≥ −2.60 (adjusted hazard ratio [aHR] 6.303), fibrosis-4 (FIB-4) score >3.25 (aHR 7.676), and MRE value ≥4.5 kPa (aHR 13.190) were associated with HCC development according to a univariate Cox proportional hazards model. A multivariate Cox proportional hazards model showed that an MRE value ≥4.5 kPa (aHR 7.301) was the only factor independently associated with HCC development. Even in patients with an FIB-4 score >3.25, the cumulative incidence rate of HCC development in those with an MRE value <4.5 kPa was significantly lower than that in patients with an MRE value ≥4.5 kPa.**

DISCUSSION: **Liver stiffness measured by MRE before DAA therapy was an excellent marker for predicting subsequent HCC development in patients with hepatitis C virus infection who achieved SVR. The same results were observed in patients with high FIB-4 scores.**

*Clinical and Translational Gastroenterology 2021;12:e00337. https://doi.org/10.14309/ctg.0000000000000337*

## INTRODUCTION

Hepatitis C virus (HCV) infection is a major global public health issue, with an estimated prevalence of 2.8% worldwide, and hepatocellular carcinoma (HCC) is the leading cause of death in patients with HCV infection (1). The introduction of oral direct-acting antivirals (DAAs) for HCV infection has dramatically increased the number of patients who are eligible for antiviral therapy, and extremely high response rates can be achieved (2,3). HCV eradication with DAA treatment also reduces liver-related morbidity, extrahepatic liver manifestations, and overall mortality (4,5). However, despite the eradication of HCV, a substantial absolute risk of HCC persists after sustained virological response (SVR), especially in patients with advanced fibrosis; therefore, continued surveillance is necessary (6–8). It is important to determine how long patients remain at high risk of HCC after SVR and for how long they might benefit from ongoing HCC surveillance in clinical practice.

Liver fibrosis stage is one of the most important factors in stratifying the risk of HCC development. The gold standard for assessing hepatic fibrosis is liver histology based on liver biopsy. However, liver biopsy is limited by its invasive nature, poor patient acceptance, and sampling errors (9–12). Several noninvasive modalities, including transient elastography (TE), magnetic resonance elastography (MRE), and serum markers such as the

[1]Department of Nursing, Faculty of Nursing, Gifu Kyoritsu University, Ogaki, Gifu, Japan; [2]Department of Gastroenterology and Hepatology, Ogaki Municipal Hospital, Ogaki, Gifu, Japan; [3]Department of Radiology, Ogaki Municipal Hospital, Ogaki, Gifu, Japan; [4]Department of Imaging Diagnosis, Ogaki Municipal Hospital, Ogaki, Gifu, Japan; [5]Department of Internal Medicine, Himeji Red Cross Hospital, Himeji, Hyougo, Japan; [6]Department of Gastroenterology and Hepatology, Nagoya University Graduate School of Medicine, Nagoya, Aichi, Japan; [7]Division of Hepatology and Pancreatology, Department of Internal Medicine, Aichi Medical University, Nagakute, Aichi, Japan; [8]Department of Epidemiology, Infectious Disease Control, and Prevention, Hiroshima University Institute of Biomedical and Health Sciences, Hiroshima, Japan. **Correspondence:** Takashi Kumada, MD, PhD. E-mail: takashi.kumada@gmail.com.
**Received September 22, 2020; accepted March 5, 2021; published online April 23, 2021**

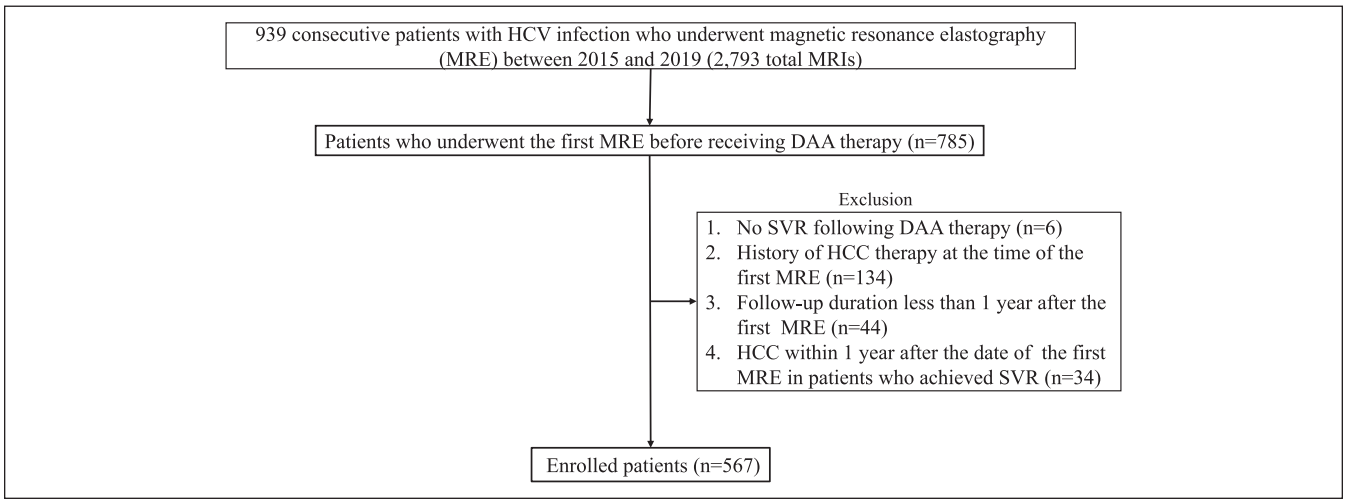


**Figure 1.** Flowchart of patient selection. DAA, direct-acting antiviral; HCC, hepatocellular carcinoma; MRI, magnetic resonance imaging; SVR, sustained virological response.

aspartate aminotransferase (AST)-to-platelet ratio index (APRI) and fibrosis-4 (FIB-4 index) (12,13), have been proposed for detecting liver fibrosis with the goal of decreasing the need for liver biopsy. MRE is an emerging technique that estimates tissue stiffness distribution using MRI-based wave imaging in the liver. Recent MRE studies reported highly accurate fibrosis detection, although there are less published data than for TE (14–17). Liver stiffness measured by MRE is a noninvasive procedure for assessing liver fibrosis stage, and it accurately detects portal hypertension (18). Liver stiffness measurement has also been proposed for evaluating the effects of antiviral treatments on liver inflammation and fibrosis, representing a possible alternative to liver histology (19).

In this study, we evaluated the usefulness of liver stiffness measured by MRE to stratify the risk of developing HCC in patients who underwent MRE before receiving DAA therapy and subsequently achieved SVR.

## MATERIALS AND METHODS

### Ethics

This cohort study, which was part of a clinical trial (study registration number UMIN000017020), was conducted to measure changes in liver stiffness using MRE in patients who achieved HCV eradication after DAA therapy. The study was approved by our Institutional Review Board (20190627-h-2) and was performed in compliance with the Helsinki Declaration. Written informed consent was obtained from all participating patients.

### Study population

A total of 939 consecutive patients with persistent HCV infection underwent MRE between 2015 and 2019 (2,793 total MRIs). Seven hundred eighty-five patients received an initial MRE before DAA therapy, and of these, 537 met the following criteria: (i) SVR after DAA therapy; (ii) no history of HCC therapy at the time of the first MRE; (iii) follow-up duration of 1 or more year after the first MRE; (iv) no HCC within 1 year after the date of the first MRE in patients who achieved SVR; and (v) no other causes of chronic liver disease (hepatotoxic drugs, autoimmune hepatitis, primary biliary cholangitis, hemochromatosis, and Wilson disease, Figure 1).

All patients were followed up at least every 6 months, and laboratory testing and ultrasound were performed at every visit. Alanine aminotransferase (ALT), AST, gamma-glutamyl transpeptidase, platelet count, albumin, total bilirubin, alkaline phosphatase, low-density lipoprotein cholesterol, high-density lipoprotein cholesterol, triglycerides, creatinine, estimated glomerular filtration rate (eGFR) (20), alpha-fetoprotein (AFP), lens culinaris agglutinin–reactive fraction of AFP (AFP-L3%), and des-carboxy prothrombin were measured at every visit. The FIB-4 index was calculated by the following formula: AST concentration (IU/L) × age (years)/(platelet count [109/L] × ALT concentration1/2 [IU/L]) (13). We used previously published cutoff values for the FIB-4. Patients with an FIB-4 value $<1.45$ were classified as having no or moderate fibrosis, while those with an FIB-4 value $>3.25$ were defined as having extensive fibrosis or cirrhosis (21). The albumin-bilirubin (ALBI) grade was calculated using the following linear equation: (log10 bilirubin μmol/L × 0.66) + (albumin/L × −0.085) (22). The continuous linear predictor was further categorized into 3 different grades for prognostic stratification purposes, as previously described: grade 1 (less than −2.60), grade 2 (between −2.60 and −1.39), and grade 3 (above −1.39) (22). AFP, AFP-L3%, and des-carboxy prothrombin were all determined using the same serum sample from each patient. The measurements of all 3 biomarkers were performed using microchip capillary electrophoresis and a liquid-phase binding assay on a μTAS Wako i30 autoanalyzer (Wako Pure Chemical Industries, Osaka, Japan) (23). Diabetes mellitus was diagnosed based on the criteria of the American Diabetes Association (24): (i) random plasma glucose ≥ 200 mg/dL, (ii) fasting plasma glucose ≥ 126 mg/dL, or (iii) use of any antihyperglycemic medications. Excessive alcohol intake was defined as consumption of more than 80 g/d of pure ethanol (25). Dyslipidemia was defined as triglycerides ≥ 150 mg/dL, high-density lipoprotein cholesterol < 40 mg/dL, low-density lipoprotein cholesterol ≥ 140 mg/dL, or treatment with lipid-lowering medication. HCC surveillance was performed every 3–6 months according to the Japanese HCC guidelines (26). The diagnosis of HCC was based on the following imaging characteristics, defined by the guidelines of the European Association for the Study of the Liver or the American Association for the Study

**Table 1. Baseline patient characteristics**

| Factors | All (n = 567) | Development of HCC | | |
|---|---|---|---|---|
| | | No (n = 549) | Yes (n = 18) | *P* |
| Age (yr) | 72 (65 to 79) | 72 (65 to 78) | 73 (67 to 81) | 0.032 |
| Sex (female) | 314 (55.4) | 306 (55.7) | 8 (44.4) | 0.349 |
| Alcohol abuse | 22 (3.9) | 22 (4.0) | 0 (0.0) | 1.000 |
| Diabetes mellitus | 398 (70.4) | 383 (70.0) | 15 (83.3) | 0.298 |
| Dyslipidemia | 389 (68.4) | 376 (68.5)/173 (31.5) | 0 (0.0) | 1.000 |
| BMI (kg/m$^2$) | 22.6 (20.5 to 25.1) | 22.6 (20.5 to 25.2) | 22.8 (20.5 to 24.2) | 0.999 |
| AST (IU/mL) | 30 (23 to 46) | 30 (23 to 45) | 32 (26 to 73.8) | 0.232 |
| ALT (IU/mL) | 25 (16 to 46) | 25 (16 to 45) | 24 (14 to 49) | 0.928 |
| Platelet count (×10$^4$/μL) | 16.5 (12.3 to 21.2) | 16.7 (12.7 to 21.2) | 12.1 (7.7 to 13.8) | <0.001 |
| FIB-4 score | 2.70 (1.85 to 4.07) | 2.63 (1.83 to 3.90) | 5.39 (4.17 to 7.96) | <0.001 |
| FIB-4 index | | | | |
| <1.45 | 82 (14.5) | 82 (14.9) | 0 (0.0) | 0.001 |
| 1.45–3.25 | 269 (47.4) | 266 (48.5) | 3 (16.7) | |
| >3.25 | 216 (38.1) | 201 (36.6) | 15 (83.3) | |
| γGTP (IU/mL) | 24 (16 to 43) | 24 (16 to 43) | 30 (18 to 46) | 0.430 |
| Total bilirubin (mg/dL) | 0.7 (0.5 to 0.9) | 0.7 (0.5 to 0.9) | 0.9 (0.6 to 1.3) | 0.015 |
| Albumin (g/dL) | 4.3 (4.1 to 4.5) | 4.3 (4.1 to 4.5) | 4.0 (3.8 to 4.2) | 0.003 |
| ALBI score | −2.97 (−3.17 to −2.74) | −3.00 (−3.17 to −2.77) | −2.66 (−2.76 to −2.35) | 0.001 |
| ALBI grade | | | | |
| 1 | 478 (85.9) | 477 (86.9) | 10 (55.6) | 0.001 |
| 2, 3 | 80 (14.1) | 72 (13.1) | 8 (44.4) | |
| ALP (IU/mL) | 258 (206 to 322) | 256 (206 to 320) | 306 (221 to 374) | 0.105 |
| HbA1c (%) | 6.0 (5.7 to 6.6) | 6.0 (5.6 to 6.5) | 6.1 (5.8 to 6.4) | 0.354 |
| Total cholesterol (mg/dL) | 222 (198 to 248) | 223 (199 to 249) | 208 (190 to 223) | 0.052 |
| Triglyceride (mg/dL) | 149 (108 to 210) | 150 (109 to 210) | 134 (96 to 201) | 0.430 |
| HDL-C (mg/dL) | 40 (33 to 49) | 40 (33 to 49) | 37 (30 to 47) | 0.496 |
| LDL-C (mg/dL) | 131 (112 to 155) | 131 (112 to 156) | 127 (102 to 140) | 0.151 |
| Creatinine (mg/dL) | 0.69 (0.59 to 0.83) | 0.68 (0.59 to 0.83) | 0.76 (0.62 to 0.89) | 0.184 |
| eGFR (mL/min/1.73 m$^2$) | 73.5 (61.0 to 86.8) | 73.6 (61.0 to 86.8) | 68.1 (61.0 to 82.2) | 0.375 |
| Genotype | | | | |
| 1 | 394 (69.5) | 379 (69.0) | 15 (83.3) | 0.258 |
| 2 | 173 (30.5) | 170 (31.0) | 3 (16.7) | |
| HCVRNA (log IU/mL) | 6.2 (5.6 to 6.5) | 6.2 (5.5 to 6.5) | 6.2 (5.8 to 6.4) | 0.835 |
| AFP (ng/mL) | 2.8 (1.8 to 5.1) | 2.8 (1.7 to 5.0) | 5.7 (3.1 to 14) | 0.004 |
| AFP-L3 (%) | 0.5 (0.5 to 0.5) | 0.5 (0.5 to 0.5) | 1.9 (0.5 to 4.9) | <0.001 |
| DCP (mAU/mL) | 15 (12 to 19) | 15 (12 to 19) | 16 (13 to 21) | 0.219 |
| First MRE value (kPa) | 3.1 (2.6 to 4.2) | 3.1 (2.5 to 4.0) | 5.6 (4.6 to 6.18) | <0.001 |
| Second MRE value (kPa) | 2.8 (2.4 to 3.7) | 2.8 (2.4 to 3.5) | 4.7 (3.4 to 5.4) | <0.001 |
| PDFF (%) | 2.2 (1.6 to 3.40) | 2.2 (1.6 to 3.5) | 2.3 (1.6 to 2.5) | 0.334 |
| PDFF > 5.2% | 72 (12.9) | 72 (13.1) | 1 (5.6) | 0.493 |

**Table 1. (*continued*)**

| Factors | All (n = 567) | Development of HCC | | |
|---|---|---|---|---|
| | | No (n = 549) | Yes (n = 18) | *P* |
| Time from first MRE to HCC diagnosis | | | 2.84 (1.82 to 3.91) | |
| Follow-up period (yr) | 3.65 (2.80 to 4.06) | 3.61 (2.72 to 4.04) | 4.20 (3.98 to 4.42) | <0.001 |

Continuous values are expressed as medians (the first to third quartiles).
AFP, alpha-fetoprotein; AFP-L3, lens culinaris agglutinin–reactive AFP; ALBI, albumin-bilirubin; ALP, alkaline phosphatase; ALT, alanine aminotransferase; AST, aspartate aminotransferase; BMI, body mass index; DCP, des-gamma-carboxy prothrombin; eGFR, estimated glomerular filtration rate; HbA1c, hemoglobin A1c; HCC, hepatocellular carcinoma; HCL-C, high-density lipoprotein cholesterol; HCVRNA, hepatitis C virus RNA; HDL, high-density lipoprotein; kPa, kilopascal; LDL-C, low-density lipoprotein cholesterol; MRE, magnetic resonance elastography; PDFF, proton density fat fraction; γGTP, gamma-glutamyl transpeptidase.

of Liver Disease: arterial hypervascularity and venous or delayed-phase washout by contrast-enhanced dynamic computed tomography or magnetic resonance imaging (27,28). Observation was started on the day of the first MRE, which was performed before DAA treatment was initiated, and was terminated on the day of HCC diagnosis or the last visit.

### Assessment of liver stiffness and steatosis using MRI

Within 4 weeks before the start of DAA therapy, all patients underwent the first MRE examination using a 3.0-T whole-body MRI system equipped with an anterior array coil as the receiver coil, and the data were analyzed by the geometry-embracing method (Discovery MR 750 W 3.0 T; GE Healthcare Japan, Tokyo, Japan). Four hundred thirty-six patients underwent the second MRE when SVR was confirmed. Liver stiffness was evaluated using MRE, which was performed as follows: Continuous longitudinal mechanical waves (60 Hz) were generated using a passive acoustic driver placed against the anterior chest wall. A two-dimensional spin-echo planar MRE sequence was used to acquire axial wave images with the following parameters: repetition time/echo time, 1,000/59.3–236 ms; continuous sinusoidal vibration, 60 Hz; field of view, 42 cm; matrix size, 64 × 64; flip angle, 90°; section thickness, 7 mm; 4 evenly spaced phase offsets; and 4 pairs of 60-Hz trapezoidal motion-encoding gradients with zeroth- and first-order moment nulling along the through-plane direction. All processing steps were automatic, with no manual intervention, and yielded quantitative images of tissue shear stiffness with measurements defined in kilopascals (kPa). On each section of the magnetic resonance magnitude image from MRE acquisition, regions of interest were drawn to include only the parenchyma of the liver, avoiding the liver edges and large blood vessels. Regions of interest also excluded areas where the phase signal-to-noise ratio (ratio of wave amplitude to noise in the wave images) was less than 5.

Liver steatosis was evaluated using the proton density fat fraction (PDFF), which was measured as described below using a modified Dixon method with advanced processing (IDEAL IQ; GE Healthcare) (29–31). A fast gradient echo sequence was used to acquire in-phase and out-of-phase images in the axial plane with the following parameters: repetition time/echo times, 7.7/1–5.1 ms; flip angle, 4°; matrix size, 160 × 160; section thickness, 7 mm; field of view, 38 cm; fractional phase field of view, 0.75–1; 1 signal acquired; bandwidth, 111.11 kHz; and imaging time, 2 breath holds (approximately 23 s each). Similar to the regions of interest drawn for liver stiffness measurements, new regions of interest were drawn on the in-phase and out-of-phase images for PDFF measurements. The PDFF was calculated as reported previously (29–31). Liver stiffness and PDFF measurements were analyzed by a radiologist (Y.S.) who specialized in hepatology and was blinded to each patient's clinical data. Regarding steatosis, the presence of fatty liver (steatosis affecting ≥ 5% of hepatocytes (32)) was defined as a PDFF ≥5.2%, based on a previous report (33). In addition, the PDFF cutoff values for diagnosing steatosis grades ≥1, ≥2, and ≥3 were 5.2%, 11.3%, and 17.1%, respectively (33). Steatosis affecting <5%, 5–33%, 33–66%, and >66% of hepatocytes was classified as grades 0, 1, 2, and 3, respectively (34).

### Statistical analysis

Continuous variables are expressed as medians (the first to third quartiles). The Mann-Whitney *U* test was used to assess continuous variables. The $\chi^2$ test with the Fisher exact test was used for categorical variables.

Univariate and multivariate Cox proportional hazards models were used to analyze factors associated with HCC development. The Cox proportional hazards models comprised the following 11 parameters: age (≥65 vs <65 years) (35), sex (female vs male), presence or absence of diabetes mellitus, presence or absence of excessive alcohol intake (pure ethanol ≥ 80 g/d), presence or absence of dyslipidemia, body mass index (≥25 vs <25 kg/m$^2$), HCV genotype (type 1 vs type 2), ALBI score (< −2.60 vs ≥ −2.60) (22), FIB-4 score (≤3.25 vs >3.25) (21), AFP (<5 vs ≥ 5 ng/mL) (36), eGFR (≥60 vs <60 mL/min/1.73 m$^2$) (20), and MRE value.

Statistical significance was defined as $P < 0.05$. All statistical analyses were performed with EZR (version 1.52, Saitama Medical Center, Jichi Medical University, Saitama, Japan), which is a graphical user interface for R (R Foundation for Statistical Computing, Vienna, Austria) (37). More precisely, it is a modified version of R commander designed to add statistical functions frequently used in biostatistics. The analysis used the survivalROC package, written using R, or performance assessment with time-dependent receiver operating characteristic (ROC) curve estimation.

## RESULTS

### Baseline characteristics of patients with and without HCC development

Table 1 shows the baseline characteristics of patients with and without HCC development. HCC was diagnosed histologically in 9 cases (resected specimens, 7 cases; liver biopsy, 2 cases) and by typical imaging findings in 9 cases (27,28). The mean maximum tumor diameter was 1.6 cm (1.0–2.3), and 17 of 18 tumors were solitary nodules. Patients without HCC development had a higher platelet count ($P < 0.001$) and albumin level ($P = 0.003$). By contrast, patients with HCC development had a higher age ($P =$

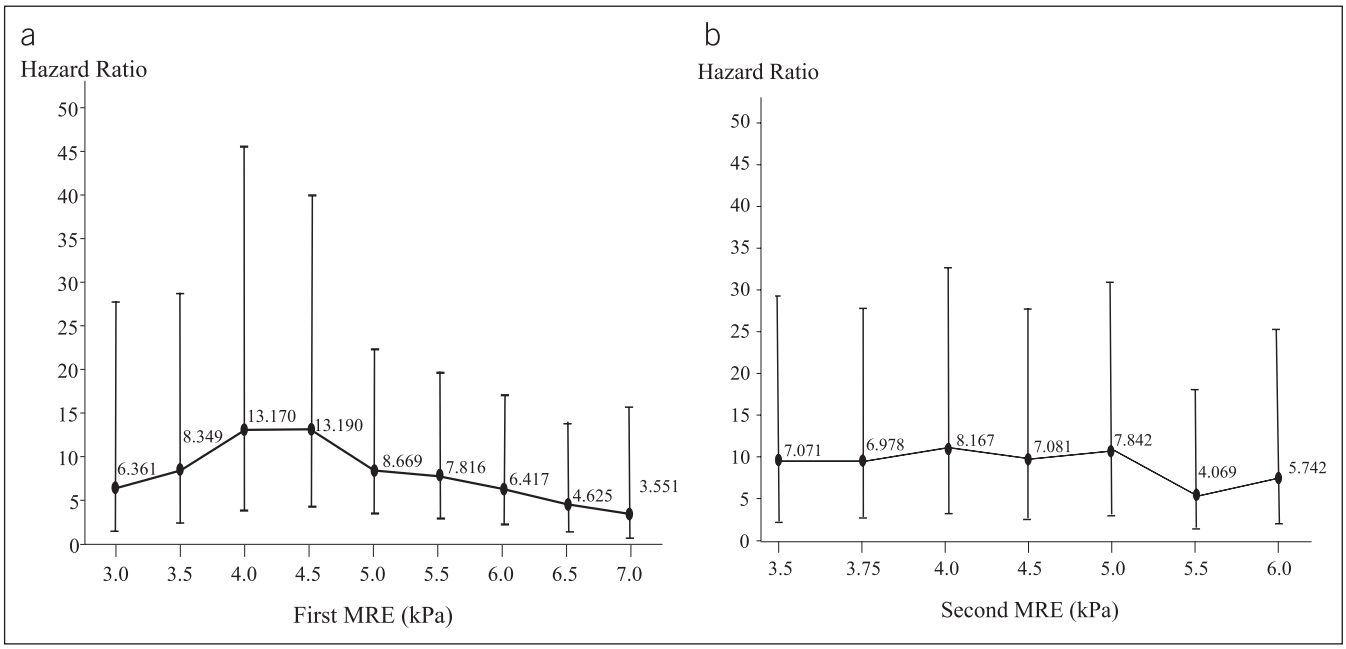


**Figure 2.** Hazard ratio of various cutoff values for the first and second MREs. (**a**) Hazard ratio of various cutoff values for the first MRE. (**b**) Hazard ratio of various cutoff values for the second MRE. MRE, magnetic resonance elastography.

0.032), FIB-4 score ($P < 0.001$), total bilirubin level ($P = 0.015$), ALBI score ($P = 0.001$), AFP level ($P = 0.004$), AFP-L3% ($P < 0.001$), and first and second MRE values ($P < 0.001$).

The optimal cutoff point of the first MRE value for predicting HCC development was determined using a univariate Cox proportional hazards model (Figure 2a). The highest hazard ratio (HR) of 13.190 (95% confidence interval [CI] 4.331–40.160, $P < 0.0001$) was achieved with a cutoff value of 4.5. The optimal cutoff point of the second MRE value for predicting HCC development was also ascertained with a univariate Cox proportional hazards model (Figure 2b). In this case, the highest HR was 8.167 (95% CI 3.063–20.340, $P < 0.0001$) when the cutoff value was 4.0. In this study, we used a first MRE value of 4.5 as the cutoff value.

Figure 3 shows the time-dependent ROC curve estimation of the MRE value and FIB-4 score at the date of the first MRE before DAA treatment. The areas under the ROC curves for the MRE value and FIB-4 score were 0.883 (95% CI 0.823–0.943) and 0.870 (95% CI 0.791–0.949) at 2 years, respectively, 0.893 (95% CI 0.845–0.940) and 0.861 (95% CI 0.794–0.928) at 3 years, respectively, and 0.858 (95% CI 0.770–0.947) and 0.818 (95% CI 0.728–0.908) at 4 years, respectively, indicating no significant difference at any time point. However, the areas under the ROC curves of the MRE value were always higher than those of the FIB-4 score.

### Factors associated with HCC development

Table 2 shows the factors associated with HCC development. The analyzed factors were age, sex, alcohol abuse, body mass index, diabetes mellitus, HCV genotype, ALBI score, FIB-4 score, AFP, eGFR, and MRE value. ALBI score $\geq -2.60$ (adjusted HR [aHR] 6.303, 95% CI 2.474–16.060, $P = 0.0001$), FIB-4 score $>3.25$ (aHR 7.676, 95% CI 2.220–26.550, $P = 0.0012$), and MRE value $\geq 4.5$ kPa (aHR 13.190, 95% CI 4.331–40.160, $P < 0.0001$) were associated with HCC development according to a univariate Cox proportional hazards model. A multivariate Cox proportional hazards model showed that an MRE value $\geq 4.5$ kPa (aHR 7.301, 95% CI 1.994–26.730, $P = 0.0027$) was the only factor that was significantly associated with HCC development.

### Cumulative incidence rates of HCC development according to MRE value

Figure 4a shows that the cumulative incidence rates of HCC development in patients whose MRE values were $<4.5$ kPa and $\geq 4.5$ kPa were 0.0% and 4.6% at 2 years, respectively, and 0.6% and 14.2% at 4 years, respectively, indicating a significant difference (log-rank test, $P < 0.0001$). Figure 4b shows that the cumulative incidence rates of HCC development in patients with an FIB-4 score $> 3.25$ and MRE values $<4.5$ kPa and $\geq 4.5$ kPa were 0.0% and 6.1% at 2 years, respectively, and 1.0% and 16.7% at

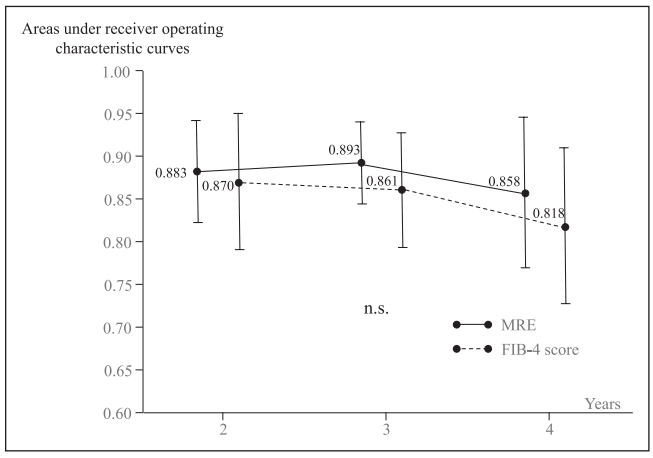


**Figure 3.** Time-dependent areas under the receiver operating characteristic curves of MRE values and FIB-4 scores. FIB-4, fibrosis-4; MRE, magnetic resonance elastography.

**Table 2. Factors associated with hepatocarcinogenesis**

| | Univariate | | | Multivariate | | |
|---|---|---|---|---|---|---|
| Factors | Crude HR | 95% CI | *P* | Adjusted HR | 95% CI | *P* |
| Age | | | | | | |
| <65 yr | 1 | | | | | |
| ≥65 yr | 1.157 | 0.421–5.046 | 0.5525 | | | |
| Sex | | | | | | |
| Female | 1 | | | | | |
| Male | 1.675 | 0.661–4.247 | 0.2773 | | | |
| Alcohol abuse | | | | | | |
| Absent | 1 | | | | | |
| Present | 0.000 | 0.000–Infinity | 0.9972 | | | |
| BMI | | | | | | |
| <25 kg/m$^2$ | 1 | | | | | |
| ≥25 kg/m$^2$ | 0.398 | 0.091–4.739 | 0.2208 | | | |
| Diabetes mellitus | | | | | | |
| Absent | 1 | | | | | |
| Present | 2.223 | 0.643–7.688 | 0.2063 | | | |
| Genotype | | | | | | |
| Type 1 | 1 | | | | | |
| Type 2 | 0.4857 | 0.140–1.685 | 0.2551 | | | |
| ALBI score | | | | | | |
| <−2.60 | 1 | | | | | |
| ≥−2.60 | 6.303 | 2.474–16.060 | 0.0001 | | | |
| FIB-4 score | | | | | | |
| ≤3.25 | 1 | | | | | |
| >3.25 | 7.676 | 2.220–26.550 | 0.0012 | | | |
| AFP | | | | | | |
| <5 ng/mL | 1 | | | | | |
| ≥5 ng/mL | 2.59 | 1.026–6.536 | 0.0439 | | | |
| eGFR | | | | | | |
| ≥60 mL/min/1.73 m$^2$ | 1 | | | | | |
| <60 mL/min/1.73 m$^2$ | 1.066 | 0.350–3.252 | 0.9103 | | | |
| MRE | | | a | | | |
| <4.5 kPa | 1 | | | 1 | | |
| ≥4.5 kPa | 13.190 | 4.331–40.160 | <0.0001 | 7.301 | 1.994–26.730 | 0.0027 |

AFP, alpha-fetoprotein; ALBI, albumin-bilirubin; BMI, body mass index; CI, confidence interval; eGFR, estimated glomerular filtration rate; HR, hazard ratio; kPa, kilopascal; MRE, magnetic resonance elastography.

4 years, respectively, indicating a significant difference (log-rank test, $P = 0.0004$). The cumulative incidence rates of HCC development in patients with an FIB-4 score ≤3.25 and MRE values <4.5 kPa and ≥4.5 kPa showed no significant difference.

## DISCUSSION

In this study, the liver stiffness value obtained by MRE was a significant predictive factor for the development of HCC. Liver stiffness as evaluated by MRE is influenced by the degree of both liver fibrosis and necroinflammatory activity. Elevated ALT levels corresponding to necroinflammatory activity are known to decline significantly from baseline to SVR (38). Therefore, Higuchi et al. (39) adopted MRE values at SVR that were minimally affected by necroinflammation and demonstrated that liver stiffness was an independent predictor of HCC development. We performed MRE before DAA therapy and at the time of SVR confirmation to determine what MRE value would be useful for predicting HCC development. The MRE value at the time of SVR

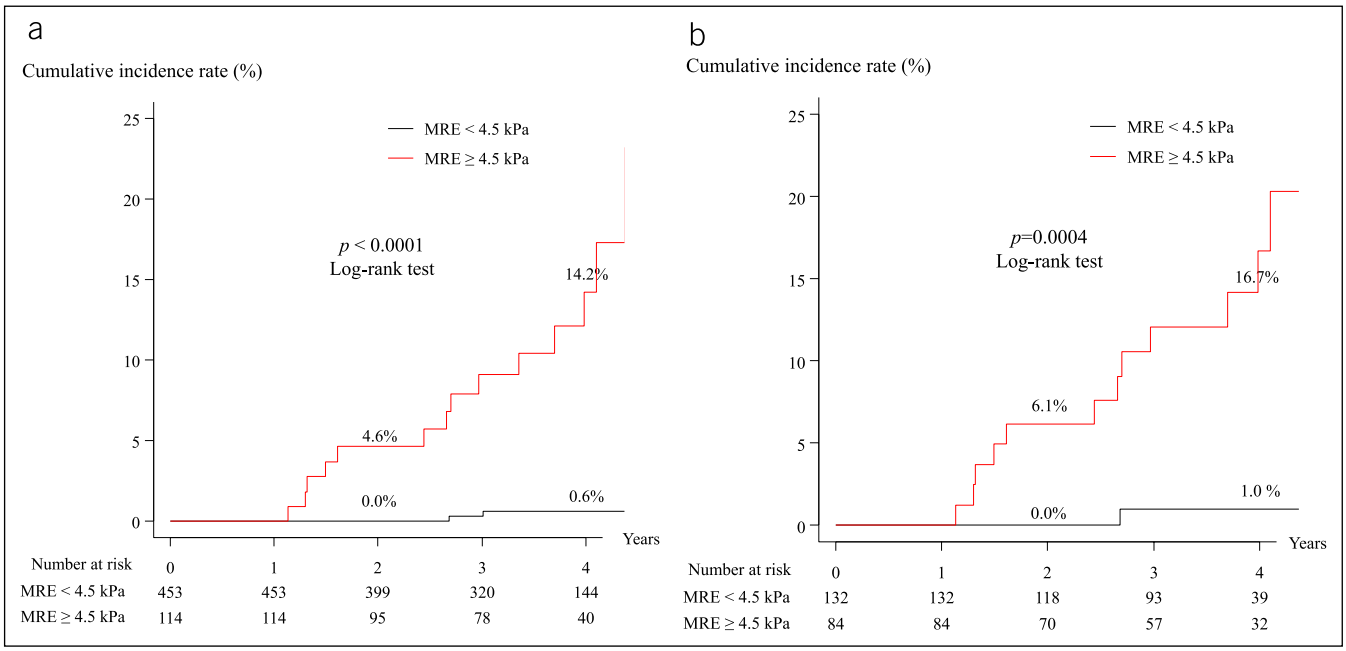


**Figure 4.** Cumulative incidence of HCC development in patients with MRE < 4.5 kPa and MRE ≥ 4.5 kPa. (**a**) All patients. (**b**) Patients with an FIB-4 score > 3.25. FIB-4, fibrosis-4; HCC, hepatocellular carcinoma; MRE, magnetic resonance elastography.

was 0.3 kPa lower than that before DAA therapy. However, there was no difference in the predictive ability between the 2 values. For this reason, we used the MRE value before DAA therapy to analyze carcinogenicity.

Several studies have reported optimum cutoff values for evaluating the degree of fibrosis and for predicting HCC development (39–41). Ichikawa et al. performed hepatic fibrosis staging with MRE using the Bayesian method (40). They proposed optimal cutoff values of 3.0 kPa for discriminating METAVIR stage ≥F2 from F0–F1, 3.7 kPa for discriminating ≥F3 from <F2, and 4.7 kPa for discriminating F4 from < F3 (42). Lee et al. (41) used the minimal *P* value approach based on the log-rank test static to determine that the cutoff stiffness values that predicted overall survival, development of hepatic decompensation, and the occurrence of HCC were 4.44 kPa, 4.46 kPa, and 5.53 kPa, respectively (41). In our study, we selected 4.5 kPa as the optimal cutoff value using univariate Cox proportional hazards models. This value is similar to that reported by Lee et al.

A univariate Cox proportional hazards model showed that the factors associated with HCC development were a high ALBI score, high FIB-4 score, and high MRE value. The ALBI score is a marker of hepatic function. In our previous study, ALBI grade 2 or 3 was associated with an increased incidence of HCC development (43). The FIB-4 score, an accurate, inexpensive, and noninvasive marker of hepatic fibrosis in HCV-infected patients, is highly advantageous in that it is available to all clinical practitioners. Many reports have suggested that the risk of HCC is positively correlated with baseline FIB-4 scores (44–46). In this study, however, a multivariate Cox proportional hazards model showed that the MRE value was the only factor associated with an increased probability of HCC development.

The cumulative incidence rate of HCC occurrence in patients with an MRE value ≥4.5 kPa was significantly higher than that in patients with an MRE value <4.5 kPa (Figure 4a), even if the FIB-4 score was >3.25 (Figure 4b). Thus, the measurement of liver stiffness by MRE was considered to be superior to the FIB-4 score, a simple and noninvasive fibrosis marker. Higuchi et al. reported that for predicting HCC development, an MRE value ≥ 3.75 kPa was associated with an HR of 5.06 (95% CI 1.42–19.1, $P = 0.01$) compared with an MRE value <3.75 kPa (39). Ichikawa et al. reported that the incidence rates of HCC development at 3 years for MRE values of <3.0 kPa, 3.0–4.7 kPa, and >4.7 kPa were 15.4%, 27.8%, and 42.7%, respectively, and there was a significant difference between groups ($P < 0.0009$) (40). By contrast, Anaparthy et al. (47) reported that there was no significant difference in liver stiffness of the background parenchyma in patients with compensated cirrhosis with or without HCC. Although the control patients with compensated cirrhosis in that report were matched with noncontrol patients by sex and disease etiology, age was not matched and follow-up results for the control patients were not shown. If close follow-up is performed in the control patients, HCC will probably occur at a high rate. Therefore, we believe that analyses that do not take temporal changes into consideration are not suitable.

MRE is currently the most accurate noninvasive technique for the detection and staging of liver fibrosis (48–50). Several studies have demonstrated that the diagnostic performance of MRE is superior to that of TE, point shear wave elastography, and two-dimensional shear wave elastography (50,51). In particular, MRE is notable for its ability to accurately diagnose mild fibrosis, which is difficult using other techniques such as TE (52). MRE results are highly reproducible and have excellent interobserver agreement, due in part to the fact that sampling error is limited by the large volume of liver that is assessed (51,53–56), and MRE findings are superior to morphological features for diagnosing cirrhosis (50,57). MRE also performs better than ultrasound elastography for diagnosing fibrosis in obese patients, with fewer non-diagnostic cases, and is able to detect fibrosis throughout the liver.

Furthermore, MRE has shown a higher technical success rate than TE.

Our study has several limitations. First, MRE has a number of drawbacks. The current clinical MRE sequence (two-dimensional gradient echo) may fail in patients with moderate to severe hepatic iron deposition, which contributed to a failure rate of 4.3% in 1 meta-analysis (50). None of the patients in this study demonstrated excessive iron deposits. MRE may also yield limited results in patients who cannot hold their breath. Breath-holding time can be reduced by decreasing the field of view or reducing the matrix size at the cost of resolution to obtain more accurate results (48). Second, the follow-up periods in this study were relatively short; their median durations in patients with and without HCC development were 2.83 years and 3.61 years, respectively. Longer follow-up periods should be used in the future. Third, MRE is more costly and time-consuming than TE and is therefore not applicable on a large scale. A simpler and more accurate method for measuring liver stiffness is needed.

In conclusion, liver stiffness measured by MRE before DAA therapy was an excellent marker for predicting subsequent HCC development in patients with HCV infection who achieved SVR, even in patients with high FIB-4 scores.

### CONFLICTS OF INTEREST

**Guarantor of the article:** Takashi Kumada, MD, PhD.

**Specific author contributions:** All authors have contributed to and agreed on the content of the manuscript. T.K., H.T., and Y.S.: concept and study design. All authors: data acquisition, review, and approval. S.T. and T.T.: data analysis. T.I. and J.T.: statistics. Y.S. and J.T.: supervision. T.K. and T.I.: manuscript preparation.

**Financial support**: This work was supported by Health and Labour Sciences Research Grants (Research on Hepatitis) from the Ministry of Health, Labour and Welfare of Japan.

**Potential competing interests:** None to report.

## Study Highlights

### WHAT IS KNOWN

- ✓ Liver fibrosis stage is one of the most important factors in stratifying the risk of developing hepatocellular carcinoma (HCC).
- ✓ Magnetic resonance elastography (MRE) is the most accurate noninvasive technique for detecting and staging liver fibrosis.

### WHAT IS NEW HERE

- ✓ A multivariate Cox proportional hazards model showed that an MRE value ≥ 4.5 kPa (adjusted hazard ratio 7.301) was significantly and independently associated with HCC development.
- ✓ The results were the same in patients with high FIB-4 scores (>3.25).

### TRANSLATIONAL IMPACT

- ✓ Liver stiffness measured by MRE before direct-acting antiviral therapy predicted HCC development in patients with hepatitis C virus infection who achieved sustained virological response.

## REFERENCES


1. Mohd Hanafiah K, Groeger J, Flaxman AD, et al. Global epidemiology of hepatitis C virus infection: New estimates of age-specific antibody to HCV seroprevalence. Hepatology 2013;57:1333–42.
2. Afdhal N, Zeuzem S, Kwo P, et al. Ledipasvir and sofosbuvir for untreated HCV genotype 1 infection. N Engl J Med 2014;370:1889–98.
3. Lawitz E, Sulkowski MS, Ghalib R, et al. Simeprevir plus sofosbuvir, with or without ribavirin, to treat chronic infection with hepatitis C virus genotype 1 in non-responders to pegylated interferon and ribavirin and treatment-naïve patients: The COSMOS randomized study. Lancet 2014; 384:1756–65.
4. van der Meer AJ, Berenguer M. Reversion of disease manifestations after HCV eradication. J Hepatol 2016;65(1 Suppl):S95–S108.
5. Janjua NZ, Chong M, Kuo M, et al. Long-term effect of sustained virological response on hepatocellular carcinoma in patients with hepatitis C in Canada. J Hepatol 2017;66:504–13.
6. Kanwal F, Kramer J, Asch SM, et al. Risk of hepatocellular cancer in HCV patients treated with direct-acting antiviral agents. Gastroenterology 2017;153:996–1005.
7. Calvaruso V, Cabibbo G, Cacciola I, et al. Incidence of hepatocellular carcinoma in patients with HCV-associated cirrhosis treated with direct-acting antiviral agents. Gastroenterology 2018;155:411–21.
8. Nahon P, Layese R, Bourcier V, et al. Incidence of hepatocellular carcinoma after direct antiviral therapy for HCV in patients with cirrhosis included in surveillance programs. Gastroenterology 2018;155:1436–50.
9. Regev A, Berho M, Jeffers LJ, et al. Sampling error and intraobserver variation in liver biopsy in patients with chronic HCV infection. Am J Gastroenterol 2002;97:2614–8.
10. Intraobserver and interobserver variations in liver biopsy interpretation in patients with chronic hepatitis C. The French METAVIR Cooperative Study Group. Hepatology 1994;20(1 Pt 1):15–20.
11. Colloredo G, Guido M, Sonzogni A, et al. Impact of liver biopsy size on histological evaluation of chronic viral hepatitis: The smaller the sample, the milder the disease. J Hepatol 2003;39:239–44.
12. Wai CT, Greenson JK, Fontana RJ, et al. A simple noninvasive index can predict both significant fibrosis and cirrhosis in patients with chronic hepatitis C. Hepatology 2003;38:518–26.
13. Sterling RK, Lissen E, Clumeck N, et al. APRICOT Clinical Investigators. Development of a simple noninvasive index to predict significant fibrosis in patients with HIV/HCV coinfection. Hepatology 2006;43:1317–25.
14. Huwart L, Sempoux C, Vicaut E, et al. Magnetic resonance elastography for the noninvasive staging of liver fibrosis. Gastroenterology 2008;135: 32–40.
15. Yin M, Talwalkar JA, Glaser KJ, et al. Assessment of hepatic fibrosis with magnetic resonance elastography. Clin Gastroenterol Hepatol 2007;5: 1207–13.
16. Bohte AE, de Niet A, Jansen L, et al. Non-invasive evaluation of liver fibrosis: A comparison of ultrasound-based transient elastography and MR elastography in patients with viral hepatitis B and C. Eur Radiol 2014; 24:638–48.
17. Yoon JH, Lee JM, Joo I, et al. Hepatic fibrosis: Prospective comparison of MR elastography and US shear-wave elastography for evaluation. Radiology 2014;273:772–82.
18. Hoffman DH, Ayoola A, Nickel D, et al. MR elastography, T1 and T2 relaxometry of liver: Role in noninvasive assessment of liver function and portal hypertension. Abdom Radiol 2020;45:2680–7.
19. Lefebvre T, Wartelle-Bladou C, Wong P, et al. Prospective comparison of transient, point shear wave, and magnetic resonance elastography for staging liver fibrosis. Eur Radiol 2019;29:6477–88.
20. Matsuo S, Imai E, Horio M, et al Collaborators developing the Japanese equation for estimated GFR. Revised equations for estimated GFR from serum creatinine in Japan. Am J Kidney Dis 2009;53:982–92.
21. Vallet-Pichard A, Mallet V, Nalpas B, et al. FIB-4: An inexpensive and accurate marker of fibrosis in HCV infection. Comparison with liver biopsy and fibrotest. Hepatology 2007;46:32–6.
22. Johnson PJ, Berhane S, Kagebayashi C, et al. Assessment of liver function in patients with hepatocellular carcinoma: A new evidence-based approach-the ALBI grade. J Clin Oncol 2015;33:550–8.
23. Kagebayashi C, Yamaguchi I, Akinaga A, et al. Automated immunoassay system for AFP-L3% using on-chip electrokinetic reaction and separation by affinity electrophoresis. Anal Biochem 2009;388:306–11.
24. American Diabetes Association. Diagnosis and classification of diabetes mellitus. Diabetes Care 2010;33:S62–9.

25. O'Shea RS, Dasarathy S, McCullough AJ. Practice guideline committee of the American association for the study of liver diseases; practice parameters committee of the American college of gastroenterology. Alcoholic liver disease. Hepatology 2010;51:307–28.
26. Kokudo N, Takemura N, Hasegawa K, et al. Clinical practice guidelines for hepatocellular carcinoma: The Japan Society of Hepatology 2017 (4th JSH-HCC guidelines) 2019 update. Hepatol Res 2019;49:1109–13.
27. European Association for the Study of the Liver. Electronic address: easloffice@easloffice.eu; European association for the study of the liver. EASL clinical practice guidelines: Management of hepatocellular carcinoma. J Hepatol 2018;69:182–236.
28. Marrero JA, Kulik LM, Sirlin CB, et al. Diagnosis, staging, and management of hepatocellular carcinoma: 2018 practice guidance by the American association for the study of liver diseases. Hepatology 2018;68:723–50.
29. Levenson H, Greensite F, Hoefs J, et al. Fatty infiltration of the liver: Quantification with phase-contrast MR imaging at 1.5 T vs biopsy. Am J Roentgenol 1991;156:307–12.
30. Bernstein MA, King KF, Zhou XJ. Handbook of MRI Pulse Sequences. San Diego, CA: Elsevier Academic Press, 2004.
31. Hussain HK, Chenevert TL, Londy FJ, et al. Hepatic fat fraction: MR imaging for quantitative measurement and display-early experience. Radiology 2005;237:1048–55.
32. Chalasani N, Younossi Z, Lavine JE, et al. The diagnosis and management of nonalcoholic fatty liver disease: Practice guidance from the American association for the study of liver diseases. Hepatology 2017;67:328–57.
33. Imajo K, Kessoku T, Honda Y, et al. Magnetic resonance imaging more accurately classifies steatosis and fibrosis in patients with nonalcoholic fatty liver disease than transient elastography. Gastroenterology 2016;150:626–37.
34. Kleiner DE, Brunt EM, Van Natta M, et al; Nonalcoholic Steatohepatitis Clinical Research Network. Design and validation of a histological scoring system for nonalcoholic fatty liver disease. Hepatology 2005;41:1313–21.
35. Foster GR, Irving WL, Cheung MC, et al. Impact of direct acting antiviral therapy in patients with chronic hepatitis C and decompensated cirrhosis. J Hepatol 2016;64:1224–31.
36. Oze T, Hiramatsu N, Yakushijin T, et al. Osaka Liver Forum. Post-treatment levels of α-fetoprotein predict incidence of hepatocellular carcinoma after interferon therapy. Clin Gastroenterol Hepatol 2014;12:1186–95.
37. Kanda Y. Investigation of the freely available easy-to-use software "EZR" for medical statistics. Bone Marrow Transpl 2013;48:452–8.
38. Ogasawara N, Kobayashi M, Akuta N, et al. Serial changes in liver stiffness and controlled attenuation parameter following direct-acting antiviral therapy against hepatitis C virus genotype 1b. J Med Virol 2018;90:313–9.
39. Higuchi M, Tamaki N, Kurosaki M, et al. Prediction of hepatocellular carcinoma after sustained virological responses using magnetic resonance elastography. Clin Gastroenterol Hepatol 2019;17:2616–8.
40. Ichikawa S, Motosugi U, Enomoto N, et al. Noninvasive hepatic fibrosis staging using mr elastography: The usefulness of the Bayesian prediction method. J Magn Reson Imaging 2017;46:375–82.
41. Lee DH, Lee JM, Chang W, et al. Prognostic role of liver stiffness measurements using magnetic resonance elastography in patients with compensated chronic liver disease. Eur Radiol 2018;28:3513–21.
42. Ishak K, Baptista A, Bianchi L, et al. Histological grading and staging of chronic hepatitis. J Hepatol 1995;22:696–9.
43. Kumada T, Toyoda H, Yasuda S, et al. Impact of the introduction of direct-acting anti-viral drugs on hepatocarcinogenesis: A prospective serial follow-up MRI study. Aliment Pharmacol Ther 2020;52:359–70.
44. Lee YB, Nam JY, Lee JH, et al. Differential effect of HCV eradication and fibrosis grade on hepatocellular carcinoma and all-cause mortality. Sci Rep 2018;8:13651.
45. Toyoda H, Tada T, Yasuda S, et al. Dynamic evaluation of liver fibrosis to assess the risk of hepatocellular carcinoma in patients with chronic hepatitis C who achieved sustained virologic response. Clin Infect Dis 2020;70:1208–14.
46. Ioannou GN, Beste LA, Green PK, et al. Increased risk for hepatocellular carcinoma persists up to 10 Years after HCV eradication in patients with baseline cirrhosis or high FIB-4 scores. Gastroenterology 2019;157:1264–78.
47. Anaparthy R, Talwalkar JA, Yin M, et al. Liver stiffness measurement by magnetic resonance elastography is not associated with developing hepatocellular carcinoma in subjects with compensated cirrhosis. Aliment Pharmacol Ther 2011;34:83–91.
48. Venkatesh SK, Ehman RL. Magnetic resonance elastography of abdomen. Abdom Imaging 2015;40:745–59.
49. Venkatesh SK, Yin M, Ehman RL. Magnetic resonance elastography of liver: Technique, analysis, and clinical applications. J Magn Reson Imaging 2013;37:544–55.
50. Singh S, Venkatesh SK, Wang Z, et al. Diagnostic performance of magnetic resonance elastography in staging liver fibrosis: A systematic review and meta-analysis of individual participant data. Clin Gastroenterol Hepatol 2015;13:440–51.
51. Guo Y, Parthasarathy S, Goyal P, et al. Magnetic resonance elastography and acoustic radiation force impulse for staging hepatic fibrosis: A meta-analysis. Abdom Imaging 2015;40:818–34.
52. Bonekamp S, Kamel I, Solga S, et al. Can imaging modalities diagnose and stage hepatic fibrosis and cirrhosis accurately? J Hepatol 2009;50:17–35.
53. Godfrey EM, Patterson AJ, Priest AN, et al. A comparison of MR elastography and 31P MR spectroscopy with histological staging of liver fibrosis. Eur Radiol 2012;22:2790–7.
54. Lee DH, Lee JM, Han JK, et al. MR elastography of healthy liver parenchyma: Normal value and reliability of the liver stiffness value measurement. J Magn Reson Imaging 2013;38:1215–23.
55. Hines CD, Bley TA, Lindstrom MJ, et al. Repeatability of magnetic resonance elastography for quantification of hepatic stiffness. J Magn Reson Imaging 2010;31:725–31.
56. Venkatesh SK, Wang G, Teo LL, et al. Magnetic resonance elastography of liver in healthy asians: Normal liver stiffness quantification and reproducibility assessment. J Magn Reson Imaging 2014;39:1–8.
57. Rustogi R, Horowitz J, Harmath C, et al. Accuracy of MR elastography and anatomic MR imaging features in the diagnosis of severe hepatic fibrosis and cirrhosis. J Magn Reson Imaging 2012;35:1356–64.